CrossMark

REPORT

Super instrumental El Niño events recorded by a *Porites* coral from the South China Sea

Xijie Wang[1,2] · Wenfeng Deng[1,3] · Xi Liu[1,2] · Gangjian Wei[1] · Xuefei Chen[1] ·
Jian-xin Zhao[3] · Guanqiang Cai[4] · Ti Zeng[5]

Abstract The 2–7-year periodicities recorded in fossil coral records have been widely used to identify paleo-El Niño events. However, the reliability of this approach in the South China Sea (SCS) has not been assessed in detail. Therefore, this paper presents monthly resolution geochemical records covering the period 1978–2015 obtained from a *Porites* coral recovered from the SCS to test the reliability of this method. The results suggest that the SCS coral reliably recorded local seawater conditions and the super El Niño events that occurred over the past 3 decades, but does not appear to have been sensitive enough to record all the other El Niños. In detail, the Sr/Ca series distinctly documents only the two super El Niños of 1997–1998 and 2014–2016 as obvious low values, but does not match the Oceanic Niño Index well. The super El Niño of 1982–1983 was identified by the growth hiatus caused by the coral bleaching and subsequent death of the coral. Three distinct stepwise variations occur in the $\delta^{13}C$ series that are coincident with the three super El Niños, which may be related to a substantial decline in endosymbiotic zooxanthellae density caused by the increase in temperature during an El Niño or the selective utilization of different zooxanthellaes that was required to survive in the extreme environment. The increase in rainfall and temperatures over the SCS during El Niños counteracts the effects on seawater $\delta^{18}O$ ($\delta^{18}O_{sw}$) and salinity; consequently, coral $\Delta\delta^{18}O$ series can be used as a proxy for $\delta^{18}O_{sw}$ and salinity, but are not appropriate for identifying El Niño activity. The findings presented here suggest that the method to identify paleo-El Niño activity based on the 2–7-year periodicities preserved in the SCS coral records might not be reliable, because the SCS is on the edge of El Niño anomalies due to its great distance from the central equatorial Pacific and the imprints of weak and medium strength El Niño events may not be recorded by the corals there.

✉ Wenfeng Deng
wfdeng@gmail.com; wfdeng@gig.ac.cn

1 State Key Laboratory of Isotope Geochemistry, Guangzhou Institute of Geochemistry, Chinese Academy of Sciences, Guangzhou 510640, Guangdong, China

2 School of Earth Science, University of Chinese Academy of Sciences, Beijing 100049, China

3 Radiogenic Isotope Facility, School of Earth and Environmental Sciences, The University of Queensland, Brisbane, QLD 4072, Australia

4 Guangzhou Marine Geological Survey, China Geological Survey, Guangzhou 510760, Guangdong, China

5 Key Laboratory of Marginal Sea Geology, Guangzhou Institute of Geochemistry, Chinese Academy of Sciences, Guangzhou 510640, Guangdong, China

Introduction

The El Niño–Southern Oscillation (ENSO) is the largest and strongest source of interannual climate variability, with a major impact on temperature and precipitation in the tropical Pacific and even on global climatic patterns, and profound global ecological, social, and economic consequences (Cane 1986). Under the background of global warming, El Niño events have become more severe and

🖄 Springer

more frequent over recent decades (Trenberth and Hoar 1996, 1997; Cai et al. 2014). For example, the three strongest El Niño events in the instrumental record (1982–1983, 1997–1998, and 2014–2016), according to the Multivariate ENSO Index (MEI) ranking (Wolter and Timlin 1998), have occurred in the space of just over 3 decades (Zhai et al. 2016; Sánchez-Murillo et al. 2017). The situation report recently released by the United Nations Food and Agriculture Organization indicated that more than 50 million people are affected by El Niño-related droughts, floods, and extreme hot and cold weather (FAO 2016). Therefore, the successful prediction of future El Niños is essential if we wish to reduce the risk of disasters resulting from these events and secure the sustainable development of human society. Physically based global circulation models have been used to successfully predict low-frequency changes in the typical El Niño indices; however, many problems remain to be addressed if we are to obtain a more complete understanding of El Niño predictability (Latif et al. 1998). Fortunately, paleoclimatic reconstruction based on the use of proxies offers an alternative approach to obtain a complete understanding of past El Niños as possible and also provides a benchmark against which to test the reliability of the climate models (Cane 2005).

There have been some robust ENSO reconstructions used by terrestrial proxies such as tree ring records (e.g., Fowler et al. 2012; Liu et al. 2017), but the most direct and reliable proxy for past El Niño events should come from the oceans since ENSO is a coupled ocean–atmosphere system. The proxy also needs to have high temporal resolution (at least monthly), because ENSO is an interannual climate variability that is characterized by monthly sea surface temperature (SST) anomalies. Considering these two factors, massive corals are undoubtedly some of the most appropriate sources of proxies used to study past El Niños because these corals incorporate isotopic and elemental tracers during the growth of their skeletons that reflect the ambient environmental conditions (Lough 2010). In addition, they contain well-defined annual bands and have high growth rates, thereby recording high resolution and dateable climate information from the surrounding seawater in which they lived (Gagan et al. 2000; Lough 2010). The Sr/Ca ratios preserved in coral skeletons have long been used to reconstruct changes in SST (Smith et al. 1979; Beck et al. 1992), and $\delta^{18}O$ values obtained from coral reflect the SST and $\delta^{18}O$ of the ambient seawater (Swart and Coleman 1980; Dunbar and Wellington 1981). Residual $\delta^{18}O$ (i.e., $\Delta\delta^{18}O$), which is calculated by subtracting the contribution of temperature from coral $\delta^{18}O$, can be used as a tracer of seawater $\delta^{18}O$ ($\delta^{18}O_{sw}$) and therefore salinity (McCulloch et al. 1994; Gagan et al. 2000; Duprey et al. 2012). The seasonal variations of coral

skeletal $\delta^{13}C$ are associated with the endosymbiotic zooxanthellae photosynthesis (Swart et al. 1996; McConnaughey et al. 1997), and the secular declining trend in coral $\delta^{13}C$ levels over the past 200 years reflects the increase in the transfer of anthropogenic CO_2 from the atmosphere to the surface oceans (Swart et al. 2010; Deng et al. 2017). Therefore, the ocean, climate, and environmental anomalies caused by El Niño can be faithfully recorded by massive corals and their geochemical proxies (e.g., McCulloch et al. 1994; McGregor and Gagan 2004; Asami et al. 2005; Kelmo et al. 2006; Quinn et al. 2006; Hereid et al. 2013; McGregor et al. 2013; Roff et al. 2015; Hetzinger et al. 2016; Ampou et al. 2017).

The South China Sea (SCS) is the largest marginal sea in the western tropical Pacific and is located on the edge of the western Pacific warm pool. Therefore, its modern interannual climate variabilities, including SST and rainfall, are controlled largely by El Niño (Wang et al. 2006; Hu et al. 2014; Wu et al. 2014; Lin et al. 2015; Tan et al. 2016). Coral reefs are widely distributed across the SCS, and their geochemical signatures have been frequently used as proxies for reconstructing past climate change, including paleo-El Niños, in this region (Yu 2012). However, these studies of paleo-El Niños based on SCS coral proxies (Peng et al. 2003; Sun et al. 2004, 2005a; Wei et al. 2007; Su et al. 2010; Song et al. 2012), along with those using proxies preserved in giant clams from the SCS (Yan et al. 2017), identified the activity of paleo-El Niños using only the 2–7-year periodic variations extracted from the time series of geochemical proxies with spectral analysis. The SCS is on the edge of El Niño anomalies due to its great distance from the central equatorial Pacific, and the influence of ENSO on the SCS SST is considered to be through the atmospheric bridge of atmospheric circulation changes (Wang et al. 2006; Rong et al. 2007). On the other hand, individual El Niño events are never exactly the same, either in terms of ocean–atmosphere anomalies or their consequences on climate anomalies; they vary at a spatiotemporal scale in terms of their intensity, spatial extent, onset, duration, and cessation (Allan et al. 1996). Therefore, the climate anomalies may respond more clearly to the super strong El Niño events such as 1982–1983, 1997–1998, and 2014–2016. Considering the above factors, the SCS may be not the best place to reconstruct the weak and medium strength El Niño events and it is necessary to ensure that the geochemical proxies are able to accurately record the El Niño signature before their utility can be widely accepted, but most previous studies did not test the reliability of the geochemical variables as El Niño proxies by comparing modern geochemical proxies with the instrumental El Niño record. Here, we use a modern *Porites* coral from the SCS, whose growth period covers the three super instrumental El Niño events (1982–1983,

1997–1998, and 2014–2016), to test the applicability and reliability of SCS coral geochemical variables as a proxy for El Niño.

Materials and methods

Coral sampling

In September 2015, a core with a diameter of 8 cm, referred to herein as 15XS1, was drilled using underwater drilling techniques from a living *Porites* sp. coral colony that had a diameter of about 2 m, from a water depth of 2.5 m on Qilianyu Reef in the Xisha Islands of the northern SCS (16°57′24.75″N, 112°18′46.80″E; Fig. 1). This core was first sectioned into slices 1-cm thick and 7–8-cm wide. Then, X-ray photographs were taken to reveal the regular and well-defined annual density bands, which were then used to establish the coral chronology (see Fig. S1 for supporting information). X-ray diffraction (XRD) analysis of the samples showed that the coral skeleton was 100% aragonite. Scanning electron microscopy (SEM) imaging revealed that there was no secondary aragonite present in the coral skeleton. Next, the coral slices were soaked in 10% H_2O_2 for 24 h to remove organic matter, and this was followed by ultrasonic cleaning at 60 kHZ and 360 W in deionized water for 30 min to remove surface contaminants. Samples were collected from the annual bands along the main growth axis using a digitally controlled milling machine. The average sampling interval for the subsamples was about 1.0–1.2 mm, which corresponded to a roughly monthly resolution during the winter periods, and about 2–3 weeks during the summer periods. The subsamples then were ground into a homogeneous fine powder (ca. 200 mesh) using an agate mortar and pestle prior to geochemical analysis.

Geochemical analysis

The coral core contained a growth hiatus, and to determine the death age of the coral, the sample from the lower surface of the growth hiatus was U–Th dated using a Nu Plasma multi-collector inductively coupled plasma mass spectrometer (MC–ICP–MS) at the Radiogenic Isotope Laboratory of The University of Queensland. A sample of approximately 0.5 g was taken from the lower surface of the growth hiatus and spiked with a ^{229}Th–^{233}U mixed tracer. The detailed analytical methods and the correction protocols used for the ^{230}Th age can be found in Clark et al. (2014).

Analysis of the Sr/Ca ratios was conducted on a Varian Vista Pro inductively coupled plasma atomic emission spectrometer (ICP-AES) at the State Key Laboratory of Isotope Geochemistry, Guangzhou Institute of Geochemistry, Chinese Academy of Sciences. The standard reference material used for calibration was the JCp-1 *Porites* sp. standard prepared by the Geological Survey of Japan (Okai et al. 2002). All Sr/Ca data were normalized against the JCp-1 standard, which has Sr/Ca = 8.838 mmol/mol (Hathorne et al. 2013). Replicate analyses of an in-house *Porites* sp. coral standard solution BH-7 showed excellent reproducibility, with an external precision of 0.16% yielding an SST error of less than 0.5 °C. Replicate measurements were made on approximately 15% of the samples.

Coral skeletal δ^{13}C and δ^{18}O analysis was performed using a GV Isoprime II stable isotope ratio mass spectrometer (IRMS) coupled with a MultiPrep carbonate

Fig. 1 Location map of study site in the SCS showing **a** the northern SCS, **b** the Xisha Islands, and **c** the Qilianyu coral reefs and sample location of the coral studied here
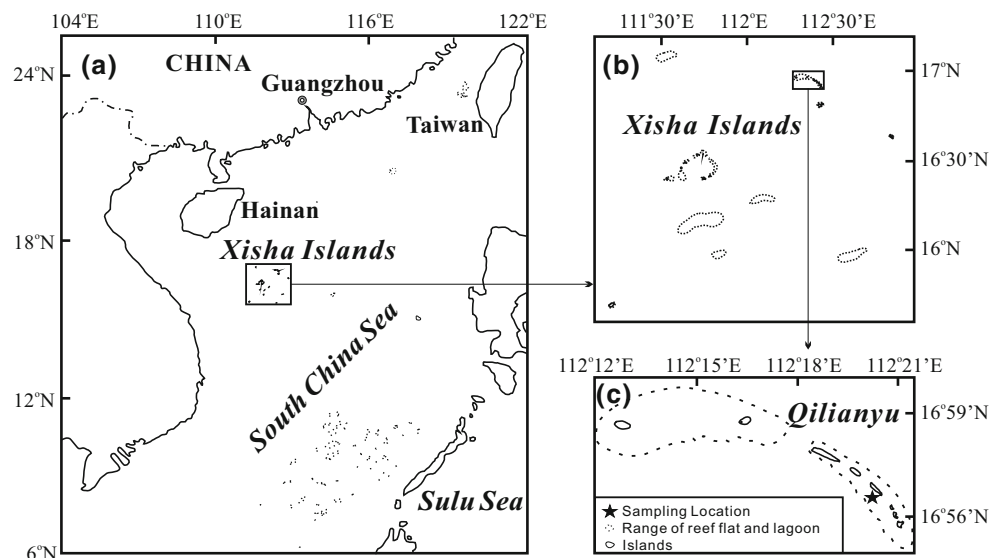
device that used 102% H_3PO_4 at 90 °C to extract CO_2 from the coral samples. The IRMS was located in the same laboratory as that used for the Sr/Ca measurements. Isotope data were normalized against the Vienna Pee Dee Belemnite (V-PDB) using the NBS-19 standard ($\delta^{13}C$ = 1.95‰, $\delta^{18}O$ = − 2.20‰). Multiple measurements of this standard yielded a reproducibility of 0.03‰ for $\delta^{13}C$ and 0.06‰ for $\delta^{18}O$. Replicate measurements were made on approximately 15% of the samples.

Coral $\Delta\delta^{18}O$, a tracer for $\delta^{18}O_{sw}$ and sea surface salinity (SSS), was calculated by subtracting the sea surface temperature (SST) contribution from the coral $\delta^{18}O$ values (McCulloch et al. 1994; Gagan et al. 2000), according to $\Delta\delta^{18}O = d\delta^{18}O/dT \times (T_{\delta18O} - T_{Sr/Ca})$, where $d\delta^{18}O/dT$ is the slope of the empirical $\delta^{18}O$–SST function obtained from the linear regression of monthly $\delta^{18}O$ and the NOAA Extended Reconstructed SST (ERSST) v4 (in situ only), and $T_{\delta18O}$ and $T_{Sr/Ca}$ are the apparent SSTs calculated from the $\delta^{18}O$ values and Sr/Ca ratios, respectively. We used the Sr/Ca–SST relationship (SST = − 18.7144 × Sr/Ca + 193.26) reported by Sun et al. (2005b).

Age model

The monthly growth chronologies of the coral were constructed using the Sr/Ca ratios, which track changes in the ambient water temperature, and assuming that each Sr/Ca cycle represents 1 year. This approach was cross-validated using visual observations of the X-radiographs and the assumption that the pairs of high- and low-density bands represent annual growth (Knutson et al. 1972; Dodge and Vaisnys 1975). Maxima in Sr/Ca ratios were assigned to the beginning of each year, which is generally the coldest period in this region. Other ages were obtained by linear interpolation (for annual cycles with < 12 data points) or nearest neighbor smoothing (for annual cycles with > 12 data points) between these age control points. The chronology of the section of core below the lower surface of the growth hiatus was established by counting the annual bands back from the U–Th dated calendar year of the lower surface. For the living part of the core above the upper surface of the growth hiatus, the chronology was established by counting the annual bands back from the youngest band, which represents the year of sampling. Calendar ages were assigned to the $\delta^{13}C$ and $\Delta\delta^{18}O$ data according to the age models outlined above based on the Sr/Ca cycles.

Spectral analysis

To identify any periodic variability within the coral records, spectral analysis was performed on the coral

geochemical series using the PAST (Paleontological Statistics) software (Hammer et al. 2001).

Climate and environmental variables

Recent instrumental climate data from the study site were unavailable; therefore, data covering the period 1978–2015 recorded at nearby stations were used in this study. The monthly SST records were extracted from the ERSST.v4 dataset on a 2° × 2° grid (cutting out region: longitude = 111.000°E, 113.000°E; latitude = 15.000°N, 17.000°N) (http://coastwatch.pfeg.noaa.gov/erddap/griddap/nceiErsstv4. html) (Huang et al. 2015). The monthly SSS records were extracted from the UK Meteorological Office EN4 (UKMO EN4) dataset on a 1° × 1° grid (cutting out region: longitude = 111.500°E, 112.500°E; latitude = 16.500°N, 17.500°N) (https://climexp.knmi.nl/select.cgi?id=someone@somewhere andfield=en4_sos) (Good et al. 2013). The Oceanic Niño Index (ONI), which is a 3-month running mean of the ERSST.v4 SST anomalies in the Niño 3.4 region (5°N–5°S, 120°W–170°W) based on centered 30-year base periods updated every 5 years (http://www.cpc.noaa.gov/products/ analysis_monitoring/ensostuff/ensoyears.shtml), was compared with the 3-month running mean of the Sr/Ca anomalies.

Results

The lower surface of the growth hiatus was dated to 33.9 ± 1.4 yr BP (Table 1), which corresponds to the Common Era year of 1982.6 ± 1.4. The recovery time of the coral was estimated to be around August of 1989 by counting the annual bands and Sr/Ca cycles back from the sampling year.

Both the coral Sr/Ca, $\delta^{13}C$ and $\delta^{18}O$ ratios show well-defined annual cycles over the study period (Fig. 2a–c). Even though the coral time series are relatively short, some statistically significant spectral peaks are able to be extracted from them (Fig. S2). However, spectral analysis revealed no significant 2–7-year ENSO periodicities at the 95% confidence level in the coral Sr/Ca, $\delta^{13}C$ and $\delta^{18}O$ records (Fig. S2a, S2b and S2c). The variations in Sr/Ca coral series are relatively stable and range from 8.631 to 9.098 mmol/mol, with an average of 8.838 mmol/mol (1SD, 0.108 mmol/mol). Coral $\delta^{13}C$ levels decrease gradually over the study period and vary between − 1.43 and − 3.95‰ with an average value of − 2.70‰ (1SD, 0.55‰). The range of the $\delta^{18}O$ values varies between − 6.27 and − 4.32‰, with an average of − 5.50‰ (1SD, 0.37‰). The annual cycles in coral $\Delta\delta^{18}O$ are not as clear as those in the coral Sr/Ca and $\delta^{13}C$ ratios (Fig. 2d), but the periodicities of approximately 2–4 years are evident in the

Table 1 Result of MC–ICP–MS U–Th dating of the death age of the coral

Sample name	U (ppm)	±2σ	^{232}Th (ppb)	±2σ	^{230}Th/^{232}Th	±2σ	^{234}U/^{238}U	±2σ	^{230}Th/^{238}U	±2σ	Uncorrected ^{230}Th age (a)	±2σ	Corrected ^{230}Th age (a)	±2σ	Initial ^{234}U/^{238}U	±2σ
15XS1	2.6428	0.0008	0.2193	0.0003	13.8	0.3	1.1460	0.00001	0.00038	0.0010	36.0	0.9	33.9	1.4	1.1460	0.0010

Ratios are activity ratios calculated from atomic ratios using the decay constants of Cheng et al. (2000). All values have been corrected for laboratory procedural blanks. Uncorrected ^{230}Th age (a) was calculated using the Isoplot/EX 3.0 program (Ludwig 2003), where 'a' denotes years. Non-radiogenic ^{230}Th correction was applied assuming non-radiogenic ^{230}Th/^{232}Th = 4.4 ± 2.2 × 10^{-6} (bulk-earth value), and that ^{238}U, ^{234}U, ^{232}Th, and ^{230}Th are in secular equilibrium. Non-radiogenic ^{230}Th correction results in large age error magnification for samples with low ^{230}Th/^{232}Th ratios

spectral analysis (Fig. S2d). The range of the $\Delta\delta^{18}$O values is very large and varies between $-$ 0.60 and 0.90‰, with an average of 0.02‰ (1SD, 0.26‰).

The δ^{18}O–SST relationship obtained from the linear regression of the monthly coral δ^{18}O and SST records was δ^{18}O $= -$ 0.142 ($\pm$0.008) $\times$ SST (°C) $-$ 1.567 ($\pm$ 0.220).

Discussion

Responses of coral records to El Niño events

Coral Sr/Ca

The coral Sr/Ca series shows a significant correlation with the SST data for the study site ($r = 0.81$, $n = 368$, $p <$ 0.0001; Fig. 3a), which indicates that coral Sr/Ca series preserves a reliable record of SST variations in the northern SCS. However, the Sr/Ca anomalies may not be a reliable proxy for El Niño events, because the 3-month running means of the coral Sr/Ca anomalies have a poor correlation with the ONI ($r = -$ 0.16, n $= 364$, $p = 0.001$) and their variation trends do not match well (Fig. 3b, c). In addition, there is no significant 2–7-year El Niño periodicity recorded in the Sr/Ca series (Fig. S2a). Therefore, the Sr/Ca series from the northern SCS may not contain a complete record of El Niño events. The SCS is not located in the core activity region of El Niño, and the climate and environment there are controlled over seasonal and inter-annual timescales by both the East Asian Monsoon and ENSO (Wang et al. 2000). The monthly Multi-scale Ultra-high Resolution (0.01°) SST near the sampling location does not correlate with the average Niño 3.4 SST well during the 2003–2015 period (Fig. S3). Moreover, the current and circulation in the upper layers of the northern SCS are affected by the seasonal coastal circulation, SCS warm current, and Kuroshio intrusion, and are therefore extremely complicated (Huang et al. 1994; Hu et al. 2000), which may affect the local seawater conditions and so weaken the imprints of El Niño preserved within the coral Sr/Ca records.

Although the coral Sr/Ca series in this study does not fully record the El Niño events preserved in the ONI, the Sr/Ca ratios from the super El Niño events of 1997–1998 and 2014–2016 are much lower than those from other years (Fig. 3b). The abnormally low coral Sr/Ca ratios correspond to the abnormally high temperatures, which agrees well with the positive SST anomalies during these two super El Niño events in the SCS (Wang et al. 2006; Zhao and Tang 2007; Chen et al. 2016). During the 1982–1983 super El Niño, there was widespread coral bleaching and significant mortality caused by thermal stress across the globe, including in the SCS (Glynn 1984, 1993; Coffroth

Fig. 2 Temporal variations of coral: **a** Sr/Ca, **b** δ¹³C, **c** δ¹⁸O and **d** Δδ¹⁸O calculated from paired Sr/Ca and δ¹⁸O series. The gray vertical bar indicates the growth hiatus. The lower surface of the growth hiatus was dated to 1982.6 ± 1.4 CE and the upper surface to approximately August 1989
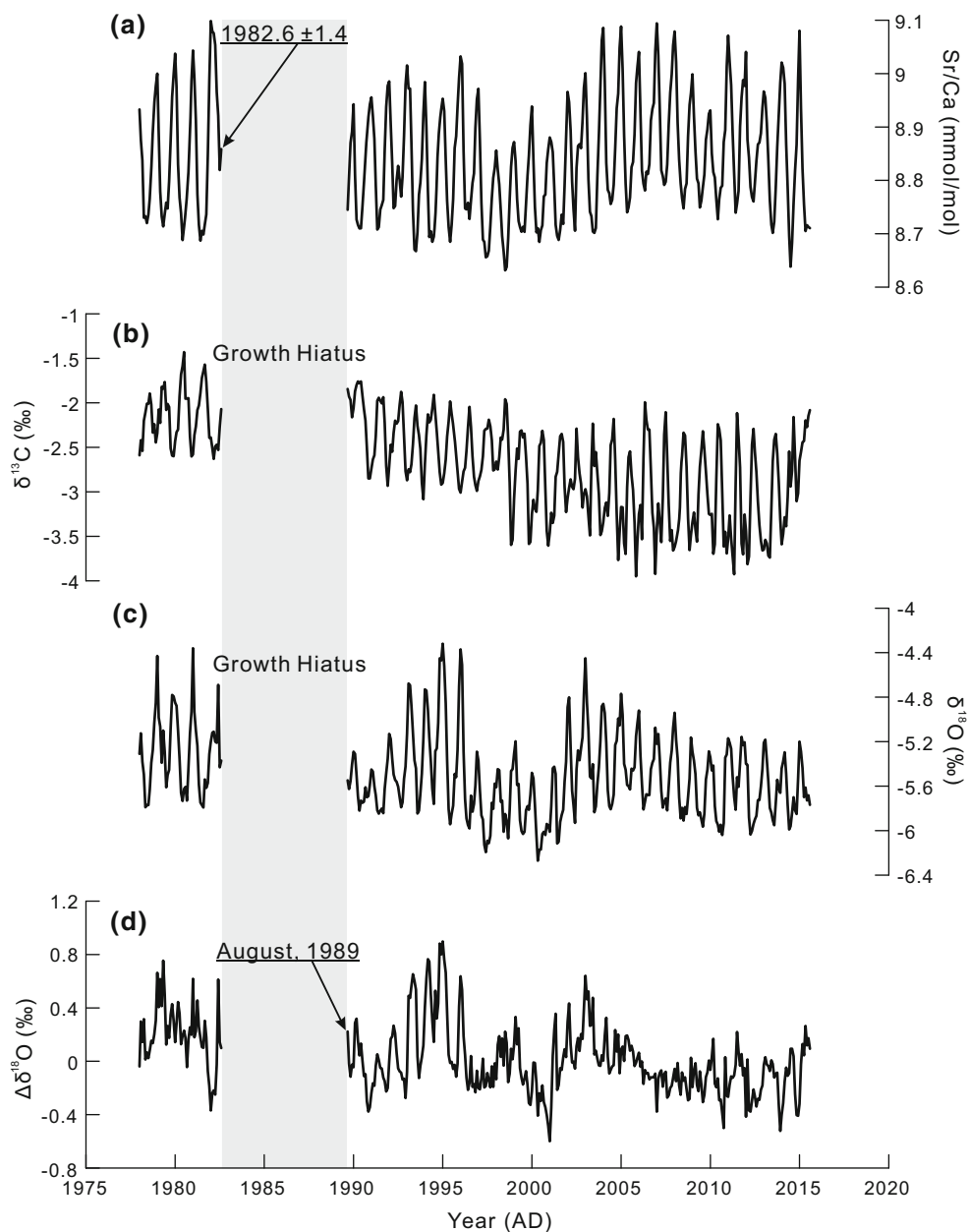
et al. 1990; Yu et al. 2006). The U–Th dating of the growth hiatus in the coral studied here shows that it too was affected by the high-temperature bleaching and died during this super El Niño event.

A recent study has indicated that warming events may change the relationship between coral Sr/Ca and temperature (Clarke et al. 2017). To evaluate the effect of El Niño events on the Sr/Ca–SST relationship, linear regression analysis was performed on these two variables during different periods before and after the three super El Niño events. The sensitivity of Sr/Ca to SST between 1978 and 1983 (i.e., before the 1982–1983 El Niño) is closely comparable (within the error range) with that between 1976

and 1994 derived from another Xisha coral (Sun et al. 2005b) (Table 2). However, this sensitivity showed a significant reduction after the recovery of the coral in 1989 and remained stable from then on. The slopes and intercepts of the Sr/Ca–SST relationships are almost identical over the periods 1989–1998 and 1999–2015, and their slopes are significantly lower than that seen during the period 1978–1983 (Table 2). Extremely high temperatures also occurred during the 1997–1998 El Niño, but the Sr/Ca–SST relationship did not change after that event. These variations in the sensitivity of Sr/Ca to SST during different periods may demonstrate that the high temperatures during El Niño events are indeed able to change the Sr/Ca–
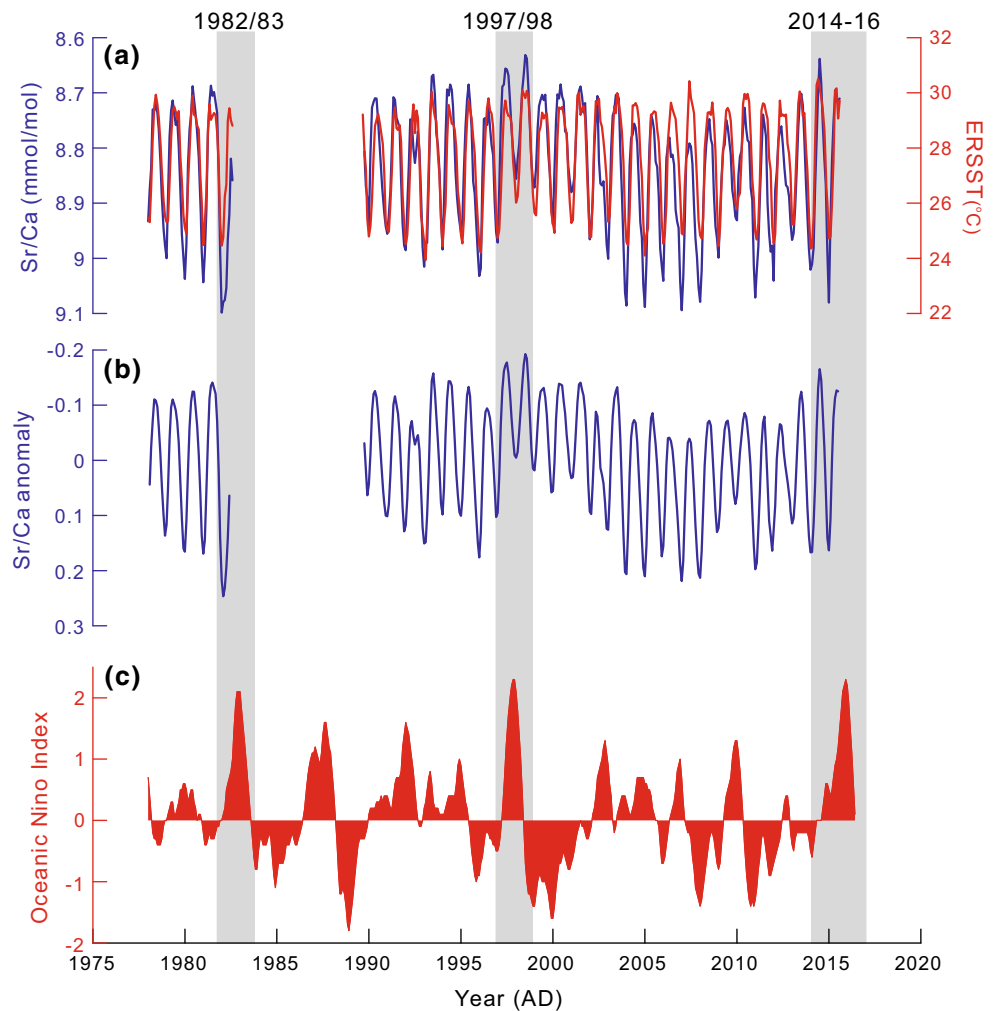
SST relationship, but this change occurs only when the extremely high temperatures lead to coral bleaching and mortality. The change in the Sr/Ca–SST relationship may be associated with the change in active transport of Ca to the site of calcification under the environmental stress (Clarke et al. 2017). The uptake of Sr into coral skeletons is affected by symbiotic zooxanthellae (Cohen et al. 2002); consequently, a change in the behavior of zooxanthellae may also lead to a change in the sensitivity of Sr/Ca to SST during El Niño events and their associated high temperatures. Even so, the variations in the Sr/Ca-SST sensitivity should be dealt with care. For one thing, the first time interval of the record covers only 5 years and the change in the Sr/Ca-SST slope could also be a statistical artifact. For another, the ERSST data do not show the extremely high temperatures during the 1997–1998 El Niño clearly (Fig. 3a). This might indicate that the ERSST does not fully resolve local SST variability. One more thing, this observation is based on only one coral colony and deserved to be cross-checked. Therefore, the Sr/Ca ratio of SCS coral may record only El Niños of a strength similar to the recent super events (ONI > 2). The effect of weaker El Niño events on SCS corals may be too subtle to affect the Sr/Ca ratios recorded in corals. The identification of paleo-El Niño activity based on the 2–7-year periodicities preserved in the coral geochemical proxies should be used cautiously because some El Niño activity might not be recorded by these proxies. To obtain reliable records of paleo-El Niño activity from fossil coral, the coral should be sampled from locations as close as possible to the Niño 3.4 region (e.g., Evans et al. 1999).

Coral $\Delta\delta^{18}O$

The $\delta^{18}O_{sw}$ and salinity series are correlated because of the similar influence of freshwater fluxes on both variables; therefore, $\delta^{18}O_{sw}$ can be used as a proxy for salinity (Rohling and Bigg 1998; Conroy et al. 2017). Furthermore, coral $\Delta\delta^{18}O$ can usually be used as a proxy for salinity because it serves as a tracer for $\delta^{18}O_{sw}$ (Corrège 2006). Coral $\Delta\delta^{18}O$ has a significant positive correlation with SSS over the periods 1978–1983 and 1989–2015 ($r = 0.38$, $n =$

368, $p < 0.0001$; Fig. 4a), which indicates that coral $\Delta\delta^{18}O$ can record partial variations in SSS. However, the correlation between SSS and ONI is poor, although significant ($r = -0.16$, $n = 364$, $p = 0.001$). Moreover, compared with the normal years, the SSS and the 3-month running means of the coral $\Delta\delta^{18}O$ anomalies show no distinctive characteristics or variations, even during the three super El Niño events (Fig. 4b, c). This relationship may indicate that the impact of El Niño events on the SSS in the northern SCS cannot be recognized immediately.

During the mature phase of El Niño, positive rainfall anomalies occur in the southern part of China and the northern SCS (Wang et al. 2000; Zhang and Sumi 2002; Wu et al. 2003), which bring more freshwater and cause the decrease in SSS. On the other hand, positive SST anomalies usually appear in the SCS during an El Niño event (Klein et al. 1999; Wang et al. 2006). The higher temperatures will enhance evaporation and increase SSS. The increased rainfall and temperatures have opposing effects on SSS and their effects on $\delta^{18}O_{sw}$ counteract each other; consequently, the imprints of El Niño preserved in coral $\Delta\delta^{18}O$ are difficult to isolate. In addition, there are three types of El Niño events (i.e., canonical El Niño, El Niño Modoki I and El Niño Modoki II) affecting climate over the SCS; their impacts on rainfall and SST anomalies over the SCS usually are not straightforward (Wang and Wang 2013; Tan et al. 2016). Therefore, although the $\Delta\delta^{18}O$ series in this SCS coral shows significant periods of 2–4 years similar to those of El Niño (Fig. S2d), it directly reflects the variations of $\delta^{18}O_{sw}$ and SSS and cannot be used to decipher the activity of El Niño.

Coral $\delta^{13}C$

The gradual decrease in coral $\delta^{13}C$ seen in this study may have been caused partly by the increase in the addition of anthropogenic $^{12}CO_2$ to the surface ocean, i.e., the oceanic ^{13}C Suess effect (Swart et al. 2010; Deng et al. 2017). However, it should be noted that there were significant negative drifts in the coral $\delta^{13}C$ after two of the super El Niño events (i.e., 1982–1983 and 1997–1998; Fig. 5a). The average coral $\delta^{13}C$ value decreased from $-2.15‰$ over the period 1978–1983, to $-2.41‰$ over the period 1989–1998, i.e., after the 1982–1983 El Niño, and then

decreased again to $-3.00‰$ over the period 1999–2015, i.e., after the 1997–1998 El Niño (Fig. 5a). Although there was little variability within these three periods, the three distinct reductions in $\delta^{13}C$ are clearly evident when viewing the whole coral $\delta^{13}C$ series (Fig. 5a). It is also interesting that the seasonal amplitude of $\delta^{13}C$ after the 1997–1998 El Niño is significantly higher than that during the period 1978–1998 (Fig. 5a). As with the coral Sr/Ca series, there is also no significant 2–7-year El Niño period preserved in the $\delta^{13}C$ series (Fig. S2b).

Previous studies have suggested that $\delta^{13}C$ values in coral skeleton are directly related to zooxanthellae density (Weil et al. 1981; Cummings and McCarty 1982) and that the photosynthesis of endosymbiotic zooxanthellae may affect coral skeletal $\delta^{13}C$ by preferentially consuming $^{12}CO_2$ and resulting in ^{13}C enrichment in the dissolved inorganic carbon in the internal calcification pool (Swart et al. 1996; McConnaughey et al. 1997). Therefore, the $\delta^{13}C$ in coral skeleton will become more negative during El Niño events because of the reduction in zooxanthellae density caused by the higher temperatures (Porter et al. 1989; Carriquiry et al. 1994; Suzuki et al. 2003). The loss of 85.8% of the symbiotic zooxanthellae will lead to a decline of 1‰ in coral $\delta^{13}C$ level (Porter et al. 1989).

Similar stepwise variations in coral skeletal $\delta^{13}C$ described above (Fig. 5a) following strong El Niño events have also been found by re-analyzing the coral data from the Hainan Island reported previously by Sun et al. (2008). There are also distinct reductions in $\delta^{13}C$ after strong El Niño events (i.e., 1972/1973, 1986–1988, and 1994/1995) (Fig. 5b, c). At the same time, the seasonal amplitudes of $\delta^{13}C$ after the most recent strong El Niño event become significantly higher afterward (Fig. 5a–c). The nature of this variation in the coral $\delta^{13}C$ record may suggest that super El Niño events cause a substantial decline in endosymbiotic zooxanthellae density, but that weaker El Niño events do not cause such major losses of zooxanthellae. However, if this is the case, the coral will eventually die because endosymbiotic zooxanthellae will become exhausted if the frequency and intensity of El Niño events increase in future. We cannot describe the state of the coral following the latest 2014–2016 super El Niño because it was sampled in 2015; however, we believe that re-investigation of this coral will be worthwhile in the future.

Table 2 Slope and intercept terms for the Sr/Ca–SST linear regressions

Period	Slope	Intercept	n	r^2	p
1978–1983	-0.060 ± 0.005	10.496 ± 0.141	56	0.72	< 0.001
1989–1998	-0.048 ± 0.003	10.144 ± 0.077	112	0.73	< 0.001
1999–2015	-0.047 ± 0.003	10.167 ± 0.069	200	0.65	< 0.001
1976–1994*	-0.053	10.327	36	0.96	< 0.001

*The Sr/Ca–SST linear regression between 1976 and 1994 was derived from Sun et al. (2005b)

Fig. 4 Comparison of coral $\Delta\delta^{18}O$ with climate variables and indexes: **a** coral $\Delta\delta^{18}O$ and UKMO EN4 SSS, **b** 3-month running means of the coral $\Delta\delta^{18}O$ anomalies, and **c** the ONI. The gray vertical bars highlight the three super El Niño events (1982–1983, 1997–1998, and 2014–2016) from the instrumental record over the past 3 decades
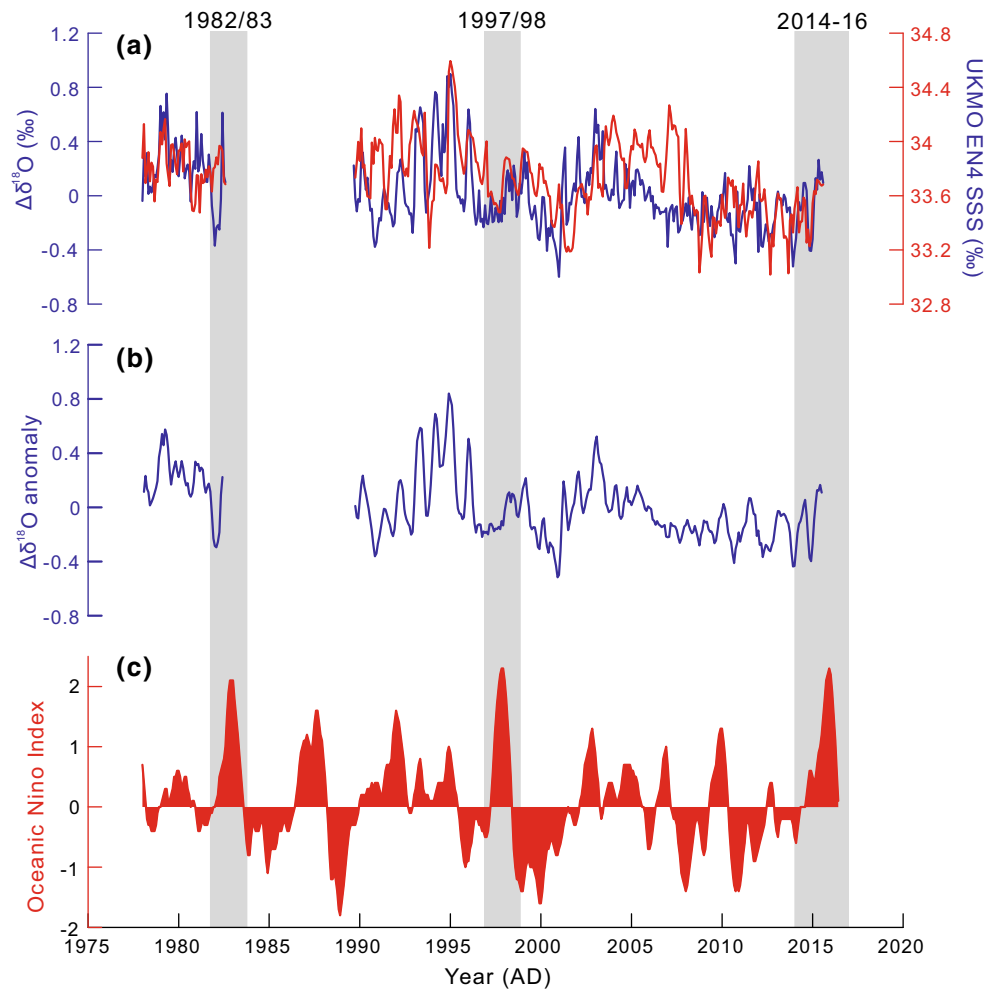
The stepwise variations in coral $\delta^{13}C$ may also be the result of a change in the physiological mechanism of the coral organism. Different types of zooxanthellae have a different ability to tolerate thermal stress (Berkelmans and van Oppen 2006); therefore, coral may selectively utilize the symbiont zooxanthellae with the higher resistance to thermal stress to survive in extreme environments. It is possible that coral contain different zooxanthellae during different periods, and that these zooxanthellaes have respective usage rate and amount when using carbon during photosynthesis, which would lead to these stepwise variations in coral skeletal $\delta^{13}C$ values over time. However, some coral species, including massive corals such as *Porites*, host almost exclusively C15-type zooxanthellae (D'Angelo et al. 2015). Therefore, further studies on coral biology are needed to confirm this assumption.

Previous studies have indicated that kinetic fractionation related to changes in growth rate played a significant role on $\delta^{13}C$ levels (McConnaughey 1989; Allison et al. 1996; Suzuki et al. 2005). On the other hand, there were decline trends in growth rates of massive *Porites* corals in the SCS

and adjacent areas in recent years (Tanzil et al. 2013; Su et al. 2016). However, another study found no relationship between growth rate or calcification and skeletal $\delta^{13}C$ in experimental corals (Swart et al. 1996). Corals growing as slowly as 1.5 mm/yr had essentially identical $\delta^{13}C$ values to portions of the same coral growing at rates of up to 8 mm/yr (Swart et al. 1996). In the present study, the studied coral has a uniform growth rate ($\sim 19 \pm 3$ mm/year) over the study period as shown in X-ray photographs (see Fig. S1 for supporting information). Therefore, the effect of growth rate on the stepwise variations in $\delta^{13}C$ levels of the coral studied here may be limited.

Coral resilience to climate change

Under the background of global warming and ocean acidification, coral bleaching events have become more frequent and more serious, and global reef ecosystems are facing the risk of extinction (Heron et al. 2016; DeCarlo et al. 2017; Hughes et al. 2017). Conversely, coral reefs have the biological ability of resilience and acclimatization

Fig. 5 Distinct stepwise variations in the $\delta^{13}C$ series from Xisha Islands (**a**) and Hainan Island (Sun et al. 2008) (**b**) and (**c**) before and after the El Niño events. The gray vertical bars highlight the three super El Niño events (1982–1983, 1997–1998, and 2014–2016) and other strong El Niño events (1972/1973, 1986–1988, and 1994/1995) from the instrumental record over the past 3 decades. The red horizontal lines indicate the averages of $\delta^{13}C$ for different periods
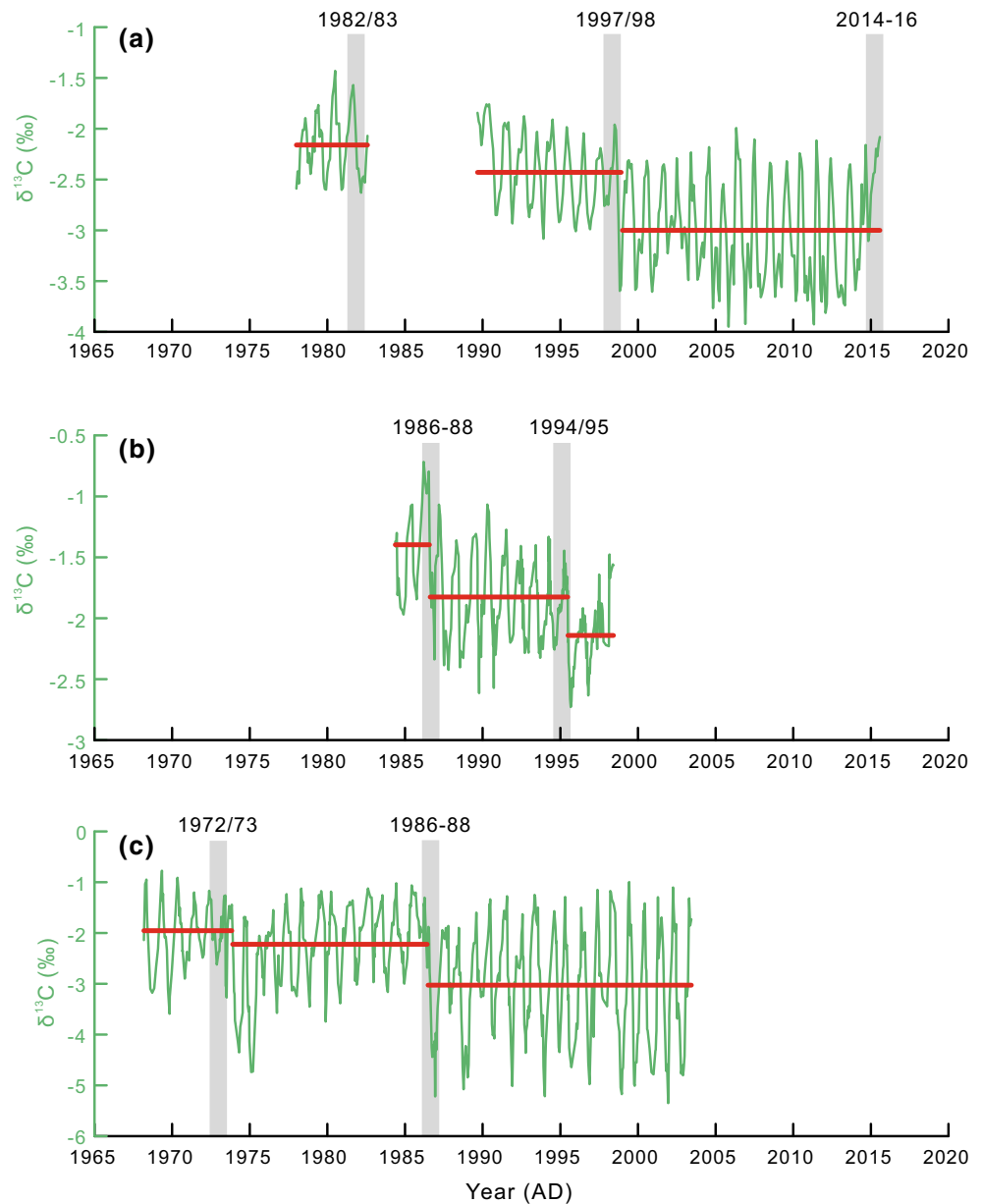
to climate change stressors (McCulloch et al. 2012; Putnam 2012; Barshis et al. 2013; van Oppen et al. 2015). The coral studied here died during the 1982–1983 El Niño, recovered around August 1989, and survived another super El Niño event, i.e., the 1997–1998 El Niño, which was stronger than the 1982–1983 event (McPhaden 1999; Enfield 2001). During the 1997–1998 event there were unprecedented numbers of reports of bleaching on many of the world's coral reefs (Lough 2000). The survival of this coral through this strong El Niño may suggest that it can adapt or acclimate to the high temperatures that occur during El Niños. The reduction in the sensitivity of Sr/Ca to SST mentioned above may be a manifestation of this self-resilience. This increased thermal tolerance may result from the change in the type of symbiont zooxanthellae in that

certain types of thermally resistant symbionts allow corals to avoid the severe bleaching of others experiencing the same stressor (Berkelmans and van Oppen 2006). Therefore, we could assist the recovery of coral reefs via the approach of human-assisted evolution, i.e., changing the taxonomic composition and density of the algal endosymbiont communities (van Oppen et al. 2015; Xu et al. 2017).

Conclusions

Based on the geochemical proxies preserved since 1978 in a *Porites* coral from the northern SCS, we studied the responses of SCS coral to El Niño events and explored the

reliability of geochemical records in the SCS coral as a proxy for El Niño. Our main conclusions are as follows.

1. The coral Sr/Ca series accurately recorded the majority of the variations in SST in the northern SCS, but only the two super El Niño events of 1997–1998 and 2014–2016 were recorded as unusually low values. As for the other super El Niño of 1982–1983, it caused coral mortality via high-temperature bleaching and the reduction in the sensitivity of Sr/Ca to SST.

2. The increased rainfall and temperatures over the northern SCS during El Niño events counteracted the effects on $\delta^{18}O_{sw}$ and SSS; consequently, the imprints of El Niño preserved in coral $\Delta\delta^{18}O$ are difficult to isolate and the SCS coral $\Delta\delta^{18}O$ is not an appropriate proxy to use in the study of El Niño activity. However, it can act as a good proxy for $\delta^{18}O_{sw}$ and SSS.

3. There were distinct stepwise variations in the coral $\delta^{13}C$ series before and after the strong El Niño events, which may be related to a substantial decline in endosymbiotic zooxanthellae density caused by the high temperatures during El Niño events. Alternatively, if the coral selectively utilizes different kinds of zooxanthellaes to survive in extreme environments, their different usage rate and amount of carbon uptake will lead to these stepwise variations in coral $\delta^{13}C$ values in different periods.

4. The method to identify paleo-El Niño activity based on the 2–7-year periodicities preserved in the SCS coral geochemical proxies should be used with caution, because the SCS is not located in the core activity region of El Niño and some El Niño activity might not be recorded by coral proxies there.

References

Allan RJ, Lindesay JA, Parker DE (1996) El Nino southern oscillation and climatic variability. CSIRO Publishing, Collingwood

Allison N, Tudhope AW, Fallick AE (1996) Factors influencing the stable carbon and oxygen isotopic composition of *Porites lutea* coral skeletons from Phuket, South Thailand. Coral Reefs 15:43–57

Ampou EE, Johan O, Menkes CE, Nio F, Birol F, Ouillon S, Andrefouet S (2017) Coral mortality induced by the 2015–2016 El-Niño in Indonesia: the effect of rapid sea level fall. Biogeosciences 14:817–826

Asami R, Yamada T, Iryu Y, Quinn TM, Meyer CP, Paulay G (2005) Interannual and decadal variability of the western Pacific sea surface condition for the years 1787–2000: Reconstruction based on stable isotope record from a Guam coral. J Geophys Res Oceans 110(C5):C05018. https://doi.org/10.1029/2004JC002555

Barshis DJ, Ladner JT, Oliver TA, Seneca FO, Traylor-Knowles N, Palumbi SR (2013) Genomic basis for coral resilience to climate change. Proc Natl Acad Sci USA 110:1387–1392

Beck JW, Edwards RL, Ito E, Taylor FW, Recy J, Rougerie F, Joannot P, Henin C (1992) Sea-surface temperature from coral skeletal strontium/calcium ratios. Science 257:644–647

Berkelmans R, van Oppen MJH (2006) The role of zooxanthellae in the thermal tolerance of corals: a 'nugget of hope' for coral reefs in an era of climate change. Proc R Soc B-Biol Sci 273:2305–2312

Cai W, Borlace S, Lengaigne M, van Rensch P, Collins M, Vecchi G, Timmermann A, Santoso A, McPhaden MJ, Wu L, England MH, Wang G, Guilyardi E, Jin F-F (2014) Increasing frequency of extreme El Niño events due to greenhouse warming. Nat Clim Chang 4:111–116

Cane MA (1986) El Niño. Annu Rev Earth Planet Sci 14:43–70

Cane MA (2005) The evolution of El Niño, past and future. Earth Planet Sci Lett 230:227–240

Carriquiry JD, Risk MJ, Schwarcz HP (1994) Stable isotope geochemistry of corals from Costa Rica as proxy indicator of the EL Niño/southern Oscillation (ENSO). Geochim Cosmochim Acta 58:335–351

Chen JP, Wen ZP, Wang X (2016) Analysis of winter and spring precipitation over Southern China during 2015/2016 extreme El Niño. Transactions of Atmospheric Sciences 39:813–826

Cheng H, Edwards RL, Hoff J, Gallup CD, Richards DA, Asmerom Y (2000) The half-lives of uranium-234 and thorium-230. Chem Geol 169:17–33

Clark TR, Zhao JX, Roff G, Feng YX, Done TJ, Nothdurft LD, Pandolfi JM (2014) Discerning the timing and cause of historical mortality events in modern *Porites* from the Great Barrier Reef. Geochim Cosmochim Acta 138:57–80

Clarke H, D'Olivo JP, Falter J, Zinke J, Lowe R, McCulloch M (2017) Differential response of corals to regional mass-warming events as evident from skeletal Sr/Ca and Mg/Ca ratios. Geochem Geophys Geosyst 18: https://doi.org/10.1002/2016gc006788

Coffroth MA, Lasker HR, Oliver JK (1990) Coral mortality outside of the eastern Pacific during 1982–1983: Relationship to El Niño. Elsevier Ocean Ser 52:141–182

Cohen AL, Owens KE, Layne GD, Shimizu N (2002) The effect of algal symbionts on the accuracy of Sr/Ca paleotemperatures from coral. Science 296:331–333

Conroy JL, Thompson DM, Cobb KM, Noone D, Rea S, LeGrande AN (2017) Spatiotemporal variability in the δ18O-salinity relationship of seawater across the tropical Pacific Ocean. Paleoceanography 32, 2016PA003073, https://doi.org/10.1002/2016pa003073

Corrège T (2006) Sea surface temperature and salinity reconstruction from coral geochemical tracers. Paleogeogr Paleoclimatol Paleoecol 232:408–428

Cummings CE, McCarty HB (1982) Stable carbon isotope ratios in *Astrangia danae*: evidence for algal modification of carbon pools used in calcification. Geochim Cosmochim Acta 46:1125–1129

D'Angelo C, Hume BCC, Burt J, Smith EG, Achterberg EP, Wiedenmann J (2015) Local adaptation constrains the distribution potential of heat-tolerant Symbiodinium from the Persian/Arabian Gulf. ISME J 9:2551–2560

DeCarlo TM, Cohen AL, Wong GTF, Davis KA, Lohmann P, Soong K (2017) Mass coral mortality under local amplification of 2 °C ocean warming. Sci Rep 7:44586

Deng W, Chen X, Wei G, Zeng T, J-x Zhao (2017) Decoupling of coral skeletal δ^{13}C and solar irradiance over the past millennium caused by the oceanic Suess effect. Paleoceanography 32:161–171. https://doi.org/10.1002/2016PA003049

Dodge RE, Vaisnys JR (1975) Hermatypic coral growth banding as environmental recorder. Nature 258:706–708

Dunbar RB, Wellington GM (1981) Stable isotopes in a branching coral monitor seasonal temperature variation. Nature 293:453–455

Duprey N, Lazareth CE, Corrège T, Le Cornec F, Maes C, Pujol N, Madeng-Yogo M, Caquineau S, Soares Derome C, Cabioch G (2012) Early mid-Holocene SST variability and surface-ocean water balance in the southwest Pacific. Paleoceanography 27:PA4207. https://doi.org/10.1029/2012PA002350

Enfield DB (2001) Evolution and historical perspective of the 1997–1998 El Niño-Southern Oscillation event. Bull Mar Sci 69:7–25

Evans MN, Fairbanks RG, Rubenstone JL (1999) The thermal oceanographic signal of El Niño reconstructed from a Kiritimati Island coral. J Geophys Res Oceans 104:13409–13421

Food and Agriculture Organization of the United Nations (2016). El Niño and La Niña: preparedness and response, situation report July 2016. (Available at http://www.fao.org/fileadmin/user_upload/emergencies/docs/FAOElNinoSitRep_versionJULY.pdf, accessed on August 12th, 2016.)

Fowler AM, Boswijk G, Lorrey AM, Gergis J, Pirie M, McCloskey SPJ, Palmer JG, Wunder J (2012) Multi-centennial tree-ring record of ENSO-related activity in New Zealand. Nature Climate Change 2:172

Gagan MK, Ayliffe LK, Beck JW, Cole JE, Druffel ERM, Dunbar RB, Schrag DP (2000) New views of tropical paleoclimates from corals. Quat Sci Rev 19:45–64

Glynn PW (1984) Widespread coral mortality and the 1982–1983 El Niño warming event. Environ Conserv 11:133–146

Glynn PW (1993) Coral reef bleaching: ecological perspectives. Coral Reefs 12:1–17

Good SA, Martin MJ, Rayner NA (2013) EN4: Quality controlled ocean temperature and salinity profiles and monthly objective analyses with uncertainty estimates. J Geophys Res Oceans 118:6704–6716

Hammer Ø, Harper DAT, Ryan PD (2001) PAST: Paleontological statistics software package for education and data analysis. Palaeontol Electron 4:1–9

Hathorne EC, Gagnon A, Felis T, Adkins J, Asami R, Boer W, Caillon N, Case D, Cobb KM, Douville E, deMenocal P, Eisenhauer A, Garbe-Schonberg D, Geibert W, Goldstein S, Hughen K, Inoue M, Kawahata H, Kolling M, Cornec FL, Linsley BK, McGregor HV, Montagna P, Nurhati IS, Quinn TM, Raddatz J, Rebaubier H, Robinson LF, Sadekov A, Sherrell R, Sinclair D, Tudhope AW, Wei GJ, Wong HR, Wu HC, You CF (2013) Interlaboratory study for coral Sr/Ca and other element/Ca ratio measurements. Geochem Geophys Geosyst 14:3730–3750. https://doi.org/10.1002/ggge.20230

Hereid KA, Quinn TM, Taylor FW, Shen CC, Edwards RL, Cheng H (2013) Coral record of reduced El Niño activity in the early 15th to middle 17th centuries. Geology 41:51–54

Heron SF, Maynard JA, van Hooidonk R, Eakin CM (2016) Warming Trends and Bleaching Stress of the World's Coral Reefs 1985–2012. Sci Rep 6:38402

Hetzinger S, Pfeiffer M, Dullo WC, Zinke J, Garbe-Schonberg D (2016) A change in coral extension rates and stable isotopes after El Niño-induced coral bleaching and regional stress events. Sci Rep 6:32879

Hu J, Kawamura H, Hong H, Qi Y (2000) A review on the currents in the South China Sea: Seasonal circulation, South China Sea warm current and Kuroshio intrusion. J Oceanogr 56:607–624

Hu WT, Wu RG, Liu Y (2014) Relation of the South China Sea precipitation variability to tropical Indo-Pacific SST anomalies during spring-to-summer transition. J Clim 27:5451–5467

Huang B, Banzon VF, Freeman E, Lawrimore J, Liu W, Peterson TC, Smith TM, Thorne PW, Woodruff SD, Zhang H-M (2015) Extended Reconstructed Sea Surface Temperature Version 4 (ERSST.v4). Part I: Upgrades and Intercomparisons. J Clim 28:911–930

Huang Q-z, Wang W-z, Li YS, Li CW (1994) Current characteristics of the South China Sea. In: Zhou D, Liang Y-B, Zeng C-K (eds) Oceanology of China Seas. Springer, Netherlands, Dordrecht, pp 39–47

Hughes TP, Kerry JT, Álvarez-Noriega M, Álvarez-Romero JG, Anderson KD, Baird AH, Babcock RC, Beger M, Bellwood DR, Berkelmans R, Bridge TC, Butler IR, Byrne M, Cantin NE, Comeau S, Connolly SR, Cumming GS, Dalton SJ, Diaz-Pulido G, Eakin CM, Figueira WF, Gilmour JP, Harrison HB, Heron SF, Hoey AS, Hobbs J-PA, Hoogenboom MO, Kennedy EV, C-y Kuo, Lough JM, Lowe RJ, Liu G, McCulloch MT, Malcolm HA, McWilliam MJ, Pandolfi JM, Pears RJ, Pratchett MS, Schoepf V, Simpson T, Skirving WJ, Sommer B, Torda G, Wachenfeld DR, Willis BL, Wilson SK (2017) Global warming and recurrent mass bleaching of corals. Nature 543:373–377

Kelmo F, Attrill MJ, Jones MB (2006) Mass mortality of coral reef ascidians following the 1997/1998 El Niño event. Hydrobiologia 555:231–240

Klein SA, Soden BJ, Lau N-C (1999) Remote sea surface temperature variations during ENSO: Evidence for a tropical atmospheric bridge. J Clim 12:917–932

Knutson DW, Buddemeier RW, Smith SV (1972) Coral Chronometers: Seasonal Growth Bands in Reef Corals. Science 177:270–272

Latif M, Anderson D, Barnett T, Cane M, Kleeman R, Leetmaa A, O'Brien J, Rosati A, Schneider E (1998) A review of the predictability and prediction of ENSO. J Geophys Res Oceans 103:14375–14393

Lin CC, Liou YJ, Huang SJ (2015) Impacts of two-type ENSO on rainfall over Taiwan. Adv Meteorol 658347

Liu Y, Cobb KM, Song H, Li Q, Li C-Y, Nakatsuka T, An Z, Zhou W, Cai Q, Li J, Leavitt SW, Sun C, Mei R, Shen C-C, Chan M-H, Sun J, Yan L, Lei Y, Ma Y, Li X, Chen D, Linderholm HW (2017) Recent enhancement of central Pacific El Niño variability relative to last eight centuries. Nature Communications 8:15386

Lough JM (2000) 1997–1998: Unprecedented thermal stress to coral reefs? Geophys Res Lett 27:3901–3904

Lough JM (2010) Climate records from corals. Wiley Interdiscip Rev-Clim Chang 1:318–331

Ludwig KR (2003). Users manual for Isoplot/Ex version 3.0: A Geochronological Toolkit for Microsoft Excel. Berkeley Geochronology Centre Special Publication No.3

McConnaughey TA (1989) ^{13}C and ^{18}O isotopic disequilibrium in biological carbonates: I. Patterns. Geochim Cosmochim Acta 53:151–162

McConnaughey TA, Burdett J, Whelan JF, Paull CH (1997) Carbon isotopes in biological carbonates: Respiration and photosynthesis. Geochim Cosmochim Acta 61:611–622

McCulloch M, Falter J, Trotter J, Montagna P (2012) Coral resilience to ocean acidification and global warming through pH up-regulation. Nat Clim Chang 2:623–627

McCulloch MT, Gagan MK, Mortimer GE, Chivas AR, Isdale PJ (1994) A High-Resolution Sr/Ca and δ^{18}O Coral Record from the Great Barrier Reef, Australia, and the 1982-1983 El-Niño. Geochim Cosmochim Acta 58:2747–2754

McGregor HV, Gagan MK (2004) Western Pacific coral δ^{18}O records of anomalous Holocene variability in the El Niño-Southern Oscillation. Geophys Res Lett 31(11):L11204. https://doi.org/10.1029/2004GL019972

McGregor HV, Fischer MJ, Gagan MK, Fink D, Phipps SJ, Wong H, Woodroffe CD (2013) A weak El Niño/Southern Oscillation with delayed seasonal growth around 4,300 years ago. Nat Geosci 6:949–953

McPhaden MJ (1999) Genesis and evolution of the 1997–1998 El Niño. Science 283:950–954

Okai T, Suzuki A, Kawahata H, Terashima S, Imai N (2002) Preparation of a new Geological Survey of Japan geochemical reference material: Coral JCp-1. Geostand Newsl 26:95–99

Peng ZC, Chen TG, Nie BF, Head MJ, He XX, Zhou WJ (2003) Coral δ^{18}O records as an indicator of winter monsoon intensity in the South China Sea. Quat Res 59:285–292

Porter JW, Fitt WK, Spero HJ, Rogers CS, White MW (1989) Bleaching in reef corals: Physiological and stable isotopic responses. Proc Natl Acad of Sci USA 86:9342–9346

Putnam HM (2012) Resilience and acclimatization potential of reef corals under predicted climate change stressors. Ph.D. thesis, University of Hawaii at Manoa

Quinn TM, Taylor FW, Crowley TJ (2006) Coral-based climate variability in the Western Pacific Warm Pool since 1867. J Geophys Res Oceans 111(C11):C11006. https://doi.org/10.1029/2005JC003243

Roff G, Zhao JX, Mumby PJ (2015) Decadal-scale rates of reef erosion following El Niño-related mass coral mortality. Glob Change Biol 21:4415–4424

Rohling EJ, Bigg GR (1998) Paleosalinity and δ^{18}O: A critical assessment. J Geophys Res Oceans 103:1307–1318

Rong Z, Liu Y, Zong H, Cheng Y (2007) Interannual sea level variability in the South China Sea and its response to ENSO. Global Planet Change 55:257–272

Sánchez-Murillo R, Durán-Quesada AM, Birkel C, Esquivel-Hernández G, Boll J (2017) Tropical precipitation anomalies and d-excess evolution during El Niño 2014-16. Hydrol Process 31:956–967

Smith SV, Buddemeier RW, Redalje RC, Houck JE (1979) Strontium-calcium thermometry in coral skeletons. Science 204:404–407

Song SH, Peng ZC, Zhou WJ, Liu WG, Liu Y, Chen TG (2012) Variation of the winter monsoon in South China Sea over the past 183 years: Evidence from oxygen isotopes in coral. Glob Planet Change 98–99:131–138

Su RX, Lough JM, Sun DH (2016) Variations in massive *Porites* growth rates at Hainan Island, northern South China Sea. Mar Ecol Prog Ser 546:47–60

Su RX, Sun DH, Chen H, Chen XM, Li ZJ (2010) Evolution of Asian monsoon variability revealed by oxygen isotopic record of middle Holocene massive coral in the northern South China Sea. Quat Int 213:56–68

Sun DH, Gagan MK, Cheng H, Scott-Gagan H, Dykoski CA, Edwards RL, Sua RX (2005a) Seasonal and interannual variability of the Mid-Holocene East Asian monsoon in coral δ^{18}O records from the South China Sea. Earth Planet Sci Lett 237:69–84

Sun DH, Su RX, McConnaughey TA, Bloemendal J (2008) Variability of skeletal growth and δ^{13}C in massive corals from the South China Sea: Effects of photosynthesis, respiration and human activities. Chem Geol 255:414–425

Sun Y, Sun M, Lee T, Nie B (2005b) Influence of seawater Sr content on coral Sr/Ca and Sr thermometry. Coral Reefs 24:23–29

Sun YL, Sun M, Wei GJ, Lee T, Nie BF, Yu ZW (2004) Strontium contents of a Porites coral from Xisha Island, South China Sea: A proxy for sea-surface temperature of the 20th century. Paleoceanography, 19(2), https://doi.org/10.1029/2003pa000959

Suzuki A, Hibino K, Iwase A, Kawahata H (2005) Intercolony variability of skeletal oxygen and carbon isotope signatures of cultured *Porites* corals: Temperature-controlled experiments. Geochim Cosmochim Acta 69:4453–4462

Suzuki A, Gagan MK, Fabricius K, Isdale PJ, Yukino I, Kawahata H (2003) Skeletal isotope microprofiles of growth perturbations in Porites corals during the 1997–1998 mass bleaching event. Coral Reefs 22:357–369

Swart PK, Coleman ML (1980) Isotopic data for scleractinian corals explain their paleotemperature uncertainties. Nature 283:557–559

Swart PK, Leder JJ, Szmant AM, Dodge RE (1996) The origin of variations in the isotopic record of scleractinian corals: II. Carbon. Geochim Cosmochim Acta 60:2871–2885

Swart PK, Greer L, Rosenheim BE, Moses CS, Waite AJ, Winter A, Dodge RE, Helmle K (2010) The ^{13}C Suess effect in scleractinian corals mirror changes in the anthropogenic CO_2 inventory of the surface oceans. Geophys Res Lett 37:L05604. https://doi.org/10.1029/2009GL041397

Tan W, Wang X, Wang W, Wang C, Zuo J (2016) Different responses of sea surface temperature in the South China Sea to various El Niño events during boreal autumn. J Clim 29:1127–1142

Tanzil JTI, Brown BE, Dunne RP, Lee JN, Kaandorp JA, Todd PA (2013) Regional decline in growth rates of massive *Porites* corals in Southeast Asia. Glob Change Biol 19:3011–3023

Trenberth KE, Hoar TJ (1996) The 1990–1995 El Niño-Southern Oscillation event: Longest on record. Geophys Res Lett 23:57–60

Trenberth KE, Hoar TJ (1997) El Niño and climate change. Geophys Res Lett 24:3057–3060

van Oppen MJH, Oliver JK, Putnam HM, Gates RD (2015) Building coral reef resilience through assisted evolution. Proc Natl Acad of Sci USA 112:2307–2313

Wang B, Wu R, Fu X (2000) Pacific-East Asian teleconnection: How does ENSO affect East Asian climate? J Clim 13:1517–1536

Wang C, Wang X (2013) Classifying El Niño Modoki I and II by different impacts on rainfall in Southern China and typhoon tracks. J Clim 26:1322–1338

Wang CZ, Wang WQ, Wang DX, Wang Q (2006) Interannual variability of the South China Sea associated with El Niño. J Geophys Res Oceans 111:C03023. https://doi.org/10.1029/2005JC003333

Wei GJ, Deng WF, Yu KF, Li XH, Sun WD, Zhao JX (2007) Sea surface temperature records in the northern South China Sea from mid-Holocene coral Sr/Ca ratios. Paleoceanography 22(3):PA3206. https://doi.org/10.1029/2006pa001270

Weil SM, Buddemeier RW, Smith SV, Kroopnick PM (1981) The stable isotopic composition of coral skeletons: control by environmental variables. Geochim Cosmochim Acta 45:1147–1153

Wolter K, Timlin MS (1998) Measuring the strength of ENSO events: How does 1997/98 rank? Weather 53:315–324

Wu R, Hu Z-Z, Kirtman BP (2003) Evolution of ENSO-related rainfall anomalies in East Asia. J Clim 16:3742–3758

Wu R, Huang G, Du Z, Hu K (2014) Cross-season relation of the South China Sea precipitation variability between winter and summer. Clim Dyn 43:193–207

Xu L, Yu K, Li S, Liu G, Tao S, Shi Q, Chen T, Zhang H (2017) Interseasonal and interspecies diversities of Symbiodinium density and effective photochemical efficiency in five dominant reef coral species from Luhuitou fringing reef, northern South China Sea. Coral Reefs 36:477–487

Yan H, Liu C, Zhang W, Li M, Zheng X, Wei G, Xie L, Deng W, Sun L (2017) ENSO variability around 2000 years ago recorded by *Tridacna gigas* δ^{18}O from the South China Sea. Quatern Int 452:148–154

Yu K-F, Zhao J-X, Shi Q, Chen T-G, Wang P-X, Collerson KD, Liu T-S (2006) U-series dating of dead *Porites* corals in the South China sea: Evidence for episodic coral mortality over the past two centuries. Quat Geochronol 1:129–141

Yu KF (2012) Coral reefs in the South China Sea: Their response to and records on past environmental changes. Sci China Earth Sci 55:1217–1229

Zhai P, Yu R, Guo Y, Li Q, Ren X, Wang Y, Xu W, Liu Y, Ding Y (2016) The strong El Niño of 2015/16 and its dominant impacts on global and China's climate. J Meteor Res 30:283–297

Zhang R, Sumi A (2002) Moisture circulation over East Asia during El Niño episode in northern winter, spring and autumn. J Meteorol Soc Jpn 80:213–227

Zhao H, Tang DL (2007) Effect of 1998 El Niño on the distribution of phytoplankton in the South China Sea. J Geophys Res Oceans 112(C2):C02017. https://doi.org/10.1029/2006JC003536